Comparison of Ray Tracing Simulations and Channel Measurements At mmWave Bands for Indoor Scenarios

Karstensen, Anders; Fan, Wei; Llorente, Ines Carton; Pedersen, Gert F.

Published in:
2016 10th European Conference on Antennas and Propagation (EuCAP)

DOI (link to publication from Publisher):
10.1109/EuCAP.2016.7481361

Publication date:
2016

Document Version
Accepted author manuscript, peer reviewed version

Comparison of Ray Tracing Simulations and Channel Measurements at mmWave bands for indoor Scenarios

Anders Karstensen, Wei Fan, Ines Carton, Gert F. Pedersen
Department of Electronic Systems, Faculty of Engineering and Science, Aalborg University, Denmark
Email: {andka, wfa, icl, gfp}@es.aau.dk

***Abstract*— Accurate characterization of spatial multipath channels at millimeter wave bands is important for system design and performance evaluation of future wireless systems. Channel measurements were conducted at two representative indoor scenarios at 26-30 GHz, i.e., a large unfurnished basement and a small furnished indoor office. A vector network analyzer connected to a rotational directional horn antenna was used in the measurements. Angle-of-arrivals and delay-of-arrivals of the multipath components were obtained from the measurements and compared with ray tracing simulations. Excellent agreement is achieved for the unfurnished basement scenario, where the same clusters were identified in the ray tracing simulations. As for the small furnished office scenario, all the dominant paths are identified as well in the ray tracing simulation, although richer multipath components in the measurement are present.**

***Index Terms*—— Ray tracing simulations, mmWave propagation, channel measurement.**

I. INTRODUCTION

To cope with the ever increasing demand for high data rates and system capacity of mobile communications, research focus is moving towards the under-utilized spectrum at millimeter wave (mmWave) frequencies [1]. Accurate radio channel characterization at these frequencies is essential for the future 5G mobile communications to become a reality.

New technologies like massive Multiple-Input Multiple-Output (MIMO) take advantage of beamforming techniques to be able to serve users in the same time-frequency slot [2, 3]. The idea is to steer the beams towards the most powerful paths reaching the user, while keeping the interference low. The question arises as how to identify these main paths. One solution is to search for the best paths by continuously steering the beams. However, this solution may fail to rapidly adapt to changes in the environment. In [4], ray tracing simulations are proposed as an alternative to beam steering in indoor scenarios. With prior knowledge of the geometry of the scenario and location of the user, ray tracing simulations can be conducted to identify potential powerful paths. This information can be stored and later used to cope with fast changes in the environment. For example, if one or more paths are blocked by a human, the beams can be directed towards other powerful paths identified by the ray tracing simulation.

Ray tracing simulations have been utilized to predict multipath propagation characteristics in mmWave bands at various propagation environments. In [5], 3D-ray tracing simulations in the urban scenarios were performed in both the 2 GHz and 28 GHz bands, where channel parameters of the radio channel model, such as path loss exponent, shadowing variance, delay spread and angle spread, were provided. In [6], 3D ray tracing simulations were performed for an outdoor scenario at mmWave bands. Ray tracing simulations and channel measurements were compared at mmWave bands to determine the importance of diffuse scattering as well in [4, 7].

In this paper, measurements at 26-30 GHz in two representative indoor scenarios are compared with ray tracing simulations. The comparison is done in terms of the power angular-delay profile. The first scenario is a large unfurnished basement where a NLOS situation is studied. On the other hand, the second scenario is a typical small furnished office. The impact of a simplified description of the environment is discussed for this scenario.

The paper is organized as follows: Section II describes the measurements setup and environments. The ray tracing tool used in the simulations as well as the simulation scenarios are introduced in section III. Section IV discusses the results obtained, whereas section V concludes the paper.

II. MEASUREMENT

A. Measurement Setup

The measurement setup consists of a wideband Biconical Tx (Transmitter) antenna, a wideband horn Rx (Receiver) antenna and the VNA (Vector Network Analyzer). As shown in Fig. 1, the received signal was down-converted to avoid excessive cable losses and phase instability. Calibration was performed up to the antennas to exclude the Tx and Rx chain from the results. The Rx antenna was mounted on a rotating pedestal, which performed a full azimuth rotation in 36 steps, with a step of 10 degrees.

The Biconical antenna has a frequency range of 2 – 30 GHz. Its radiation pattern is close to omnidirectional in the azimuth plane, and its gain is approximately 5.5 dBi at 26-30 GHz. The horn antenna has a frequency range of 26 – 40 GHz, with HPBW (Half Power Beam Width) about 21 degrees for E-plane and H-plane at 26 – 30 GHz and a gain of approximately 18.5 dBi. Both antennas are vertically polarized.

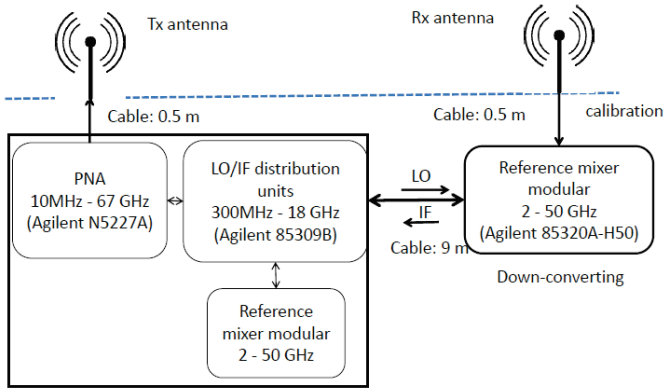

Fig. 1. System overview of measurement setup

Measurements were performed in two different rooms, namely, a large empty basement and a small office. In the basement, a bandwidth of 2 GHz centered around 29 GHz was used, giving a delay resolution of 0.5 ns. Moreover, 750 frequency points were used in the measurements limiting the maximum delay to 375 ns or a maximum distance of 112.5 m. In the small office, to have finer resolutions in delay domain to identify multipath components, a bandwidth of 4 GHz centered on 28 GHz was used, which results in a delay resolution of 0.25 ns. In this case, 1500 frequency points were selected. That is, we have a maximum delay of 375 ns as well.

Note that both Tx and Rx antennas were placed at the same height during the measurements, with 81 cm for the empty room and 91 cm for the small furnished office, respectively.

B. Measurement environments

As previously mentioned, measurements were performed in a large empty basement and a small office. Pictures of these environments are shown in Fig. 2 and Fig. 3, respectively.

The large empty room shown in Fig. 2 is a very open room located in a basement. Floor, ceiling and walls are made of thick and solid concrete. There are a few wooden doors along the corridor wall. There is also a small window and metal radiator on the wall opposite to the corridor. However, those small details are not modeled in the ray tracing simulations, as explained later. Note that a non-line of sight scenario was selected in the measurement, as shown in Fig. 2 and Fig.4.

In the small furnished office shown in Fig. 3, there are several desks, chairs and monitors, as well as wooden cabinets next to the desks. Metal shelves and a whiteboard are mounted on the wall, resulting in areas with different reflection coefficients than the drywall. The Rx antenna was placed close to the windows, whereas the Tx antenna was placed close to the center of the room as illustrated in Fig. 3 and Fig.5. This location was measured in three different scenarios.

- LOS
- Obstructed LOS with metal block; a metal plate of 42cmx42cm was placed to block the LOS between Rx and Tx.
- Obstructed LOS with human block; the metal plate was replaced by a person to block the LOS at the same location.

Fig. 2. Large empty room, NLOS measurement a) Tx viewpoint towards Rx b) Rx viewpoint towards Tx

Fig. 3 Small furnished office a) View from window corner. b) view from open door entering the office.

III. RAY TRACING SETUP

A. Ray Tracing modelling

The 3D ray tracing tool "3D Scat" implemented by Bologna University was used in the study [8, 9]. The two rooms are modelled in the Ray tracing tool, both with a simplified description of the environment. The large empty room consists mainly of walls, ceiling and floor made from concrete. Details such as wooden doors, a small window and the ventilation tubes in the ceiling are not modeled. This leaves a very simple model of the room as is shown in Fig.4.

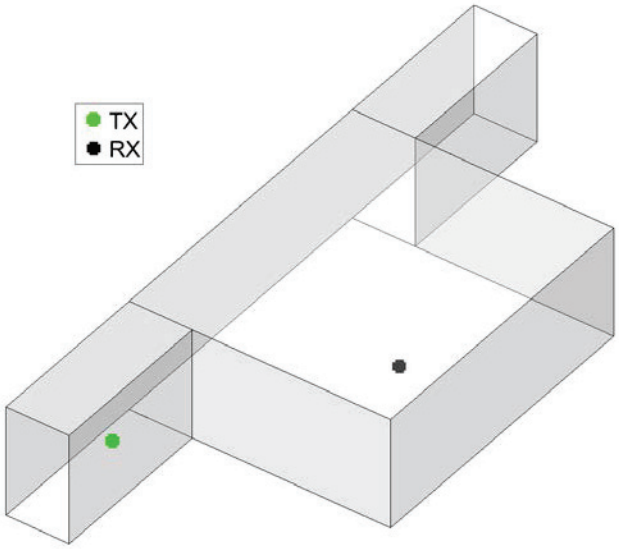

Fig. 4. Perspective view of large empty room

The smaller office environment was modeled with larger details such as wooden desks, windows, wooden cabinets, monitors, whiteboards and metallic shelves. Structural simplifications include but are not limited to chairs, keyboards, books and curtains. The modeled details of the small office are shown in Fig.5.

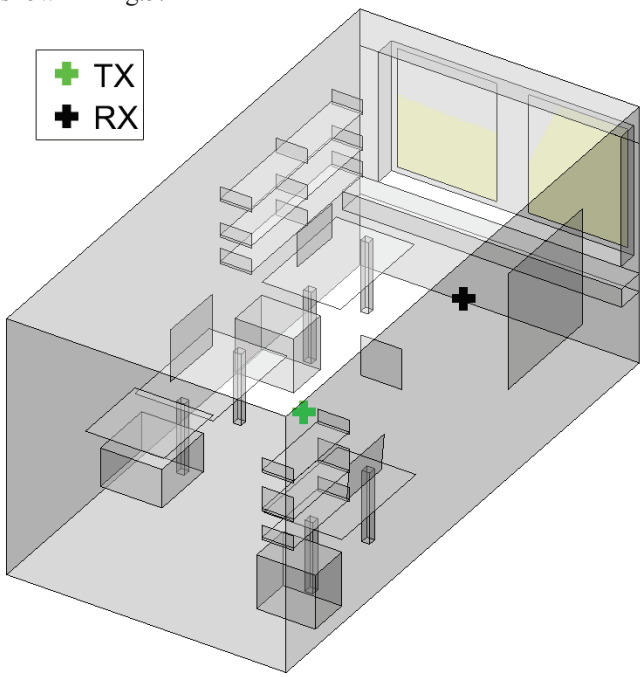

Fig. 5. Perspective view of the small office and the modeled furniture.

B. *Simulation parameters*

Both simulations include only specular reflections and diffractions. The maximum number of total interactions is set to 6, with a maximum of 6 reflections and 2 diffractions. A restriction of 4 interactions applies when there is both reflection and diffraction in the same ray. A power threshold is set to 200 dB. Note that diffuse scattering effect was not considered in the investigation in the paper.

IV. Result Comparison

A. *Large emtpy room*

Fig.6 shows the power-angular-delay profile for the measurements and the ray tracing simulation in the large empty room. Although some clusters (paths with similar angles and delay) can be identified, the measured power-angular-delay profile is quite sparse in both delay and angle domains, with only a few dominant paths. We can see that measurements and simulations show a remarkable agreement, where most paths within 35 dB dynamic range were identified in the ray tracing simulations. An illustration of the path trajectories in the ray tracing tool is shown in Fig. 7. The paths in the first two clusters are spread in delay, which is caused by the reflections back and forth inside the corridor before entering the open area. This also causes a small spread in the angular domain for the clusters. The paths from the third cluster are similar to the first two clusters. However, it is formed by two different path trajectories as shown in Fig.7. The paths in the fourth cluster are more limited in both delay and angle as all rays have very similar trajectories, as shown in Fig 7.

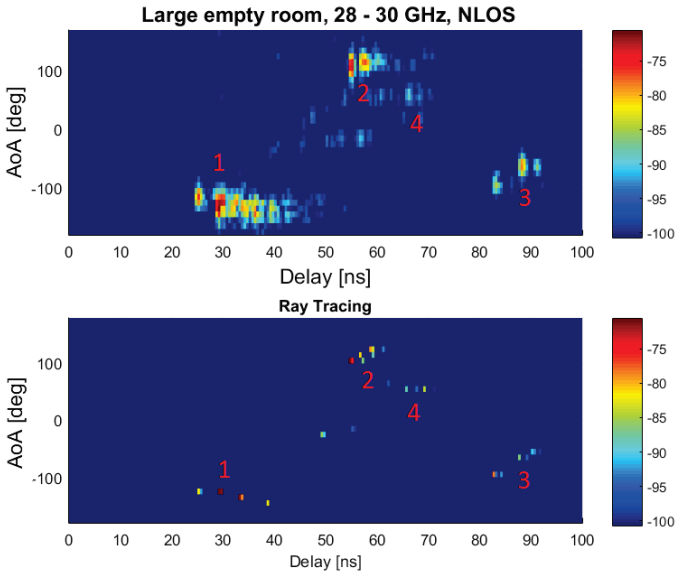

Fig. 6. Measured power-angular-delay profile (up) and simulated power-angular-delay profile (below) in the basement.

B. *Small office*

The measured power-angular-spectrum for the three scenarios for the small office is shown in Fig. 8. As we can see, multipath components identified in the LOS and O-LOS (metallic block and human block) scenarios are quite similar, except the paths impinging the Rx in LOS directions, which are blocked.

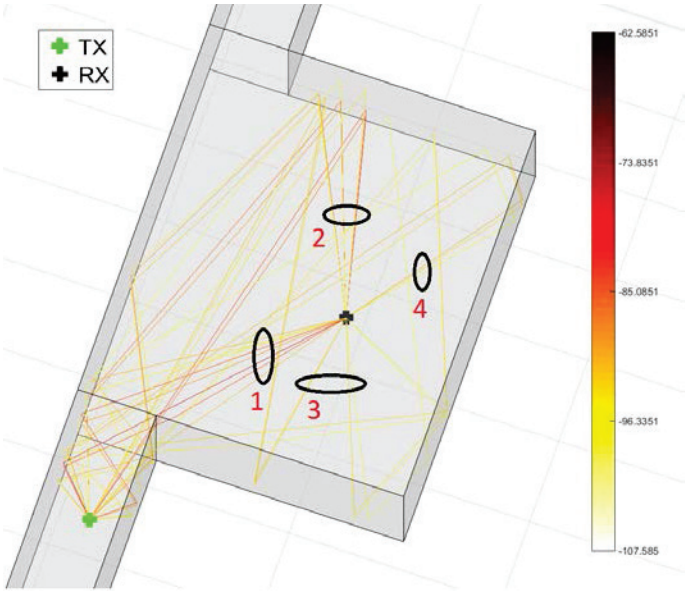

Fig.7 Rays and numbered clusters from large empty room simulation.

In Fig. 8, the first arriving components with human and metal obstruction are compared to the non-obstructed LOS measurement. The person, which is blocking the LOS component, attenuates the first arriving component from -47.1 to -62.7 dB. The person is then replaced by a metal plate, and further attenuates the first arriving component to -68.7 dB. Though physically smaller than the human, the metal plate is a better block, with 6 dB more attenuation than the human. It can be seen in Fig. 8 that the first arriving component at -90 degree and some reflections directly behind the Rx at 90 degree around 14 and 16.5 ns are attenuated by the obstruction. Paths of other angles are not affected as they are not blocked by the obstruction.

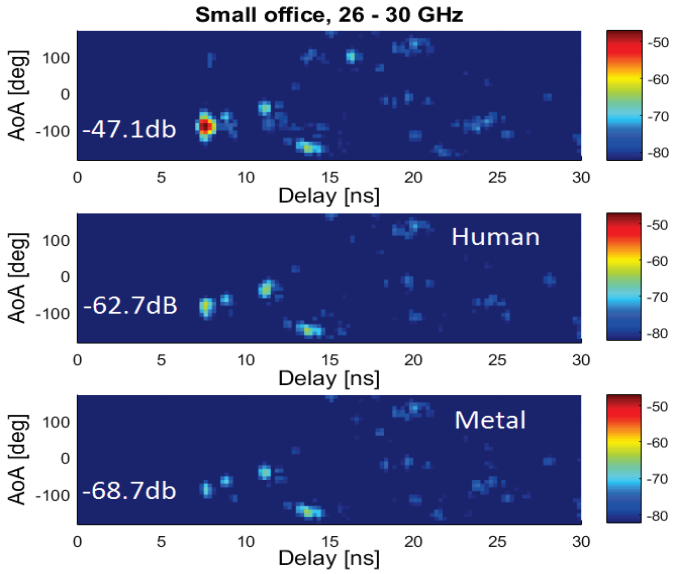

Fig. 8. a) LOS without obstruction. b) LOS obstructed by human. c) LOS obstructed by metal plate.

In Fig. 9 the power-angular-delay profile for an obstructed NLOS scenario (with metallic block) in the small office measurement is shown. Note that the power dynamic range is set according to the measurement results. In spite of being more difficult to identify specific trajectories in this scenario, the strongest ones, numbered 1-5, are all present in the ray tracing simulated results. These trajectories are also marked and numbered in Fig. 10, where the rays from the simulation are shown. These trajectories are easily recognizable and match the measurements in both angle and delay domains. If we compare the power of the paths in the measurements to the ray tracing simulation, we can see that is fits closely for several paths, yet not for all of them. This could be a consequence of the simplification of the model or a mismatch of the material properties applied. There are two paths right behind the first arriving component at around 8-9 ns. These paths are the two most significant trajectories missing in the simulation. This is due to the fact that these paths come from the chairs in front of the desks, which were not modeled.

Moreover, a richer multipath environment can be observed for the measured results, with many more paths present in the delay and angle domain. This might be due to a stronger diffuse scattering from objects, which is not modeled in the ray tracing simulation. This effect will be further investigated in future work.

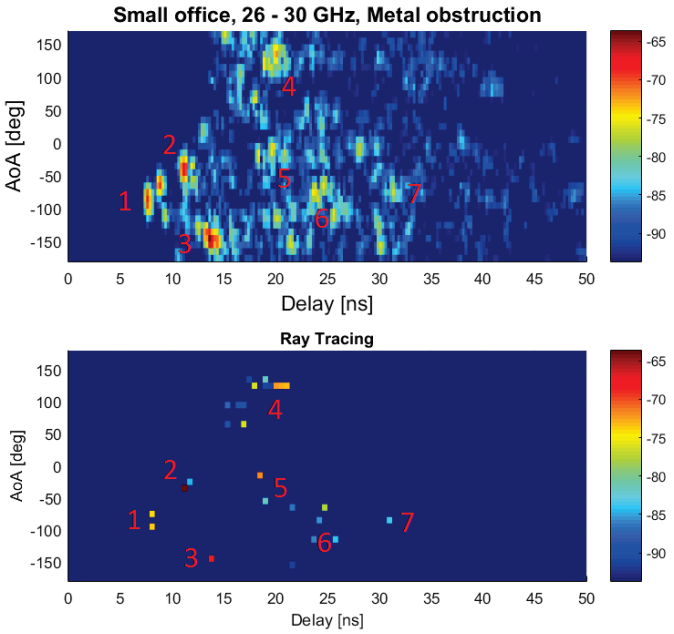

Fig. 9. Measured power-angular-delay profile (up) and simulated power-angular-delay profile (below) in the small furnished office with the metal plate blocking the LOS component.

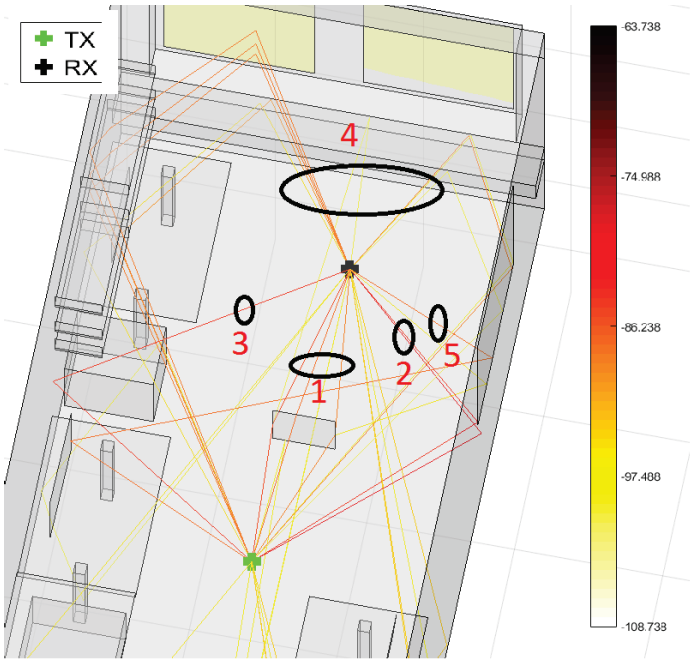

Fig.10 Rays and numbered clusters from the small office simulation.

V. CONCLUSION

In this paper, we have compared the angular-delay power spectrum extracted from measurements at mmWave frequencies with ray tracing simulations for two different indoor environments, namely a big empty room and a small furnished office.

In the large empty room, the measurement was performed in a NLOS situation. Results show that the most powerful paths were grouped in clusters in the measurements. The agreement achieved with the ray tracing simulation is remarkable, as all clusters and paths trajectories were successfully identified. In the small furnished office, the comparison between the measurements and ray tracing simulations using the metallic block to obstruct the LOS component has been shown as well. In this case, some of the furniture was modeled in the simulation. The most dominant components are identified by the simulation, and only a couple of dominant paths are missing due to the simplification of the model. Further investigation is necessary to determine whether one or more factors can further improve the results. Possible causes of the mismatch are lack of detail in the model, the absence of diffuse scattering or mismatch of the material properties.

ACKNOWLEDGMENT

This work has been supported by the Danish High Technology Foundation via the VIRTUOSO project. The authors appreciate the assistance from Kristian Bank and Kim Olesen with the practical measurements. The authors would like to thank Dr. Vittorio Degli-Esposti and Dr. Enrico Maria Vitucci for providing the "3D Scat" ray tracing tool.

REFERENCES

[1] T.S. Rappaport, S. Sun, R. Mayzus, H. Zhao, Y. Azar, K. Wang, G.N. Wong, J.K. Schulz, M. Samimi, F. Gutierrez, "*Millimeter Wave Mobile Communications for 5G Cellular: It Will Work!*", IEEE Access, Vol. 1, pp. 335-349, May, 2013.

[2] E. G. Larsson, F. Tufvesson, O. Edfors, and T. L. Marzetta, Massive MIMO for Next Generation Wireless Systems, IEEE Commun. Mag., vol. 52, no. 2, pp. 186-195, Feb. 2014.

[3] Lu Lu; Li, G.Y.; Swindlehurst, A.L.; Ashikhmin, A.; Rui Zhang, "An Overview of Massive MIMO: Benefits and Challenges," in Selected Topics in Signal Processing, IEEE Journal of , vol.8, no.5, pp.742-758, Oct. 2014.

[4] V. Degli-Esposti, F. Fuschini, E.M. Vitucci, M. Barbiroli, M. Zoli, L. Tian, X. Yin, D.A. Dupleich, R. Muller, C. Schneider, R.S. Thoma, "*Ray-Tracing-Based mm-Wave Beamforming Assessment*", IEEE Access, Vol. 2, pp. 1314-1325, October, 2014.

[5] Sooyoung Hur; Sangkyu Baek; ByungChul Kim; JeongHo Park; Molisch, A.F.; Haneda, K.; Peter, M., "28 GHz channel modeling using 3D ray-tracing in urban environments," in Antennas and Propagation (EuCAP), 2015 9th European Conference on , vol., no., pp.1-5, 13-17 April 2015

[6] Kimura, Kazunori, and Jun Horikoshi. "Prediction of millimeter-wave multipath propagation characteristics in mobile radio environment." IEICE transactions on electronics 82.7 (1999): 1253-1259.

[7] M. T. Martínez-Inglés, D. P. Gaillot, J. Pascual-García, J. M. Molina-Garcia-Pardo, J. M. Lienard and J. V. Rodriguez, "Deterministic andExperimental Indoor mmW Channel Modeling", IEEE Antennas and Wireless Propagation Letters, vol. 13, pp. 1047-1050, 2014.

[8] F. Fuschini, H. El-Sallabi, V. Degli-Esposti, L. Vuokko, D. Guiducci, and P. Vainikainen, "Analysis of multipath propagation in urban environment through multidimensional measurements and advanced ray tracing simulation," Antennas and Propagation, IEEE Transactions on, vol. 56, no. 3, pp. 848–857, March 2008.

[9] V. Degli-Esposti, D. Guiducci, A. de'Marsi, P. Azzi, and F. Fuschini, "Anadvanced field prediction model including diffuse scattering," Antennas and Propagation, IEEE Transactions on, vol. 52, no. 7, pp. 1717–1728, July 2004.